Title
Isosorbide telechelic bio-based oligomers

Journal
Journal of Polymer Science Part A Polymer Chemistry, 55(13)

ISSN
0887-624X

Authors
Rodier, Jean-David
D'Anna, Vincenza
Ritter, Nicolas
et al.

Publication Date
2017-07-01

DOI
10.1002/pola.28603

Peer reviewed

Isosorbide telechelic bio-based oligomers

J.-D. Rodier,[a,b] V. D'Anna,[c] N. Ritter,[b] S. Dalicieux,[b] C. Chamignon,[a] P. Sautet,[c] J.-P. Pascault,[a] A. Rousseau[a] and E. Fleury[a].

[a] Université-Lyon, INSA-Lyon, Ingénierie des Matériaux Polymères, IMP, UMR 5223, 69621 Villeurbanne, France

[b] Gattefossé SAS, 69804 Saint-Priest, France

c Université de Lyon, CNRS, Ecole Normale Supérieure de Lyon, Laboratoire de Chimie, UMR 5182, 69342 Lyon, France.

Abstract

The paper describes i) the structural characterization of copolymers obtained by acid catalyzed polymerization of renewable monomers: 1,3-propanediol (PDO) and isosorbide ii) the mechanism of etherification between isosorbide and PDO and transetherification between isosorbide and the homopolymer of PDO, polytrimethylene ether glycol (PTEG). Both experimental and computational approaches were considered.

The structures of the synthesized co-oligomers are determined through 2D-NMR techniques: ^{1}H-^{13}C Heteronuclear Single Quantum Coherence (HSQC), ^{1}H-^{13}C and Heteronuclear Multiple Bond Correlation (HMBC), and COSY ^{1}H-^{1}H. The molar mass, the degree of polymerization and the chain-ends of the oligomers (PDO or isosorbide unit) were obtained through ^{1}H-NMR. MALDI-TOF mass spectrometry is a complementary tool to corroborate the structures. Differential Scanning Calorimetry (DSC) and Thermogravimetric Analysis gave the first basic thermal properties of the synthesized oligomers, glass transition temperature Tg and thermal stability. DSC measurements show an increase of the copolymers' Tg compared to PDO homopolymers. The analytical data as a whole revealed that, in our experimental conditions, the synthesized copolymers are low molar mass polymers terminated by isosorbide units, despite the presence of two hydroxyl groups on each isosorbide monomer. These structures and the limited molar mass measured suggest the coexistence of etherification and transetherification reactions evolving respectively the 5 (endo) and 2 (exo) hydroxyl functions of the isosorbide. Some copolymers containing 23 to 38 mole % of isosorbide in the polymer coupled with a molar mass ($\overline{M}_n$) lower than 610 g.mol-1 show good water solubility at 1wt-%. Density Functional Theory (DFT) calculations were performed in order to obtain more insight on the reactivity and the mechanisms. The presence of the solvent was considered, and the thermodynamic of the system was evaluated at the experimental temperature of reaction (150 °C).

1 Introduction

Energetic and economic biorefinery models are proposed to produce chemical building blocks from carbohydrates as major renewable resources.[1] Indeed, biorefinery processes present the advantages of producing high quality renewable monomers, which are directly usable to produce bio-based polymers with a low carbon foot-print.

For example, fermentation of starch leads to the production of glycerol possibly convertible into 1,2 propanediol, acrylic acid and 1,3-propanediol (PDO).[2-6] PDO can be converted into polymers by melt condensation to produce polyurethanes or polyesters (Sorona®) or fully renewable materials such as polytrimethylene ether glycol (PTEG). This polyether was firstly prepared at the end of the 40's[7] and in the 60's.[8] Thirty years later, efforts have been made by DuPont to produce and commercialize the PTEG, under the trade name Cerenol™.[9,10] Today PTEG is used as raw material for application such as personal care ingredient,[11-13] as heat transfer fluid[14] or as a macrodiol for polyurethanes[15] and polyesters,[16] in coating, adhesives, sealant and elastomers.[17] PDO monomer may be condensed in a melted state through the dehydration of hydroxyl functions in presence of an acid catalyst: sulfuric acid or 1,1,2,2-tetrafluoroethanesulfonic acid (TFESA).[10,18] The mechanism of polymerization involves a SN_1 step where hydroxyl chain ends are protonated then dehydrated and a SN_2 second step where the protonated hydroxyl chain ends acts as a leaving group during nucleophilic attack of other hydroxyl chain ends.[19,20] The presence of these cationic intermediates lead the formation of side-products like propanal or unsaturated ends.[19] Using sulfuric acid also leads to the formation of sulfate esters. Temperature, nature and amount of catalyst, nitrogen flow, etc. are parameters which have been deeply studied and optimized to limit these side-reactions.[19-21]

The solubility of PTEG in water depends on its molar mass. Whereas 1,3-propanediol and low PTEG molar mass are soluble in water, PTEG with $\overline{M}_n$ superior to 300 g.mol-1 present a hydrophobic behavior. In addition, water solubility is temperature dependent. Thus an oligomer with $\overline{M}_n$ ~300 g.mol-1 (corresponding to 4.8 repeating 1,3-propanediol units) is soluble in water under 15 and above 60 wt-% at room temperature. Increasing temperature above 40°C, the solution turns into two phases due to the LCST (Lower Critical Solubility Temperature) properties.[22]

In order to adjust the PTEG solubility in aqueous media, hydrophilic reagents such as ethylene glycol (EG) or polyethylene glycol (PEG) were copolymerized with PDO leading to copolymers having a higher affinity with water.[23] However, with EG and PEG high reaction temperatures (170°C) were required, leading to the formation of toxic by-products, such as 1,4-dioxane.

Isosorbide is another renewable monomer obtained from the bioconversion of starch. The double dehydration of sorbitol[24] give two fused tetrahydrofuran rings (Figure 1a), conferring a high hydrophilicity to isosorbide.[25,26] It is recognized as a monomer for future green polymers and is already valorized in commercial polymers such as polycarbonate Durabio™.[27,28] Isosorbide was also reacted with some short alkyl chain reagents (bromobutane, bromopentane or bromohexane…) to yield hydrotropes or non-ionic surfactant monoethers.[25,29] To enhance their hydrophilic character, it was possible to modify the 2-O position of the latter products by adding glyceryl of triethylene glycol groups. Polyethers of isosorbide were firstly described by Morrison, in combination with epichlorohydrin.[30] After that, many polyethers have been prepared by using epoxy derivatives or dihalogenated compounds.[31-33] Poly(isosorbide-alkylene-ether) have been described with various methylene repeating units (m = 4, 6, 8, 10 and 12)[32,33] (Figure 1b).

(a) (b)

Figure 1: Structures of isosorbide (a) and poly(isosorbide-alkylene-ether) (b)

The present work aims to study the synthesis of novel oligoethers based on 1,3-propanediol and isosorbide, which has never been described before, to our knowledge. Two processes were explored: the first is the reaction between the PDO and isosorbide (**Process A**), while in the second process PTEG oligomers and isosorbide were used as reagent (**Process B**). The microstructure of the oligoethers was then carefully characterized and the results were discussed in the light of the theoretical calculations based on the Density Functional Theory (DFT) aiming at the rationalization of the thermodynamics of the processes. Furthermore the thermal and solubility properties of the oligoethers were then systematically compared with those of PTEG oligomers.

2 Experimental

Chemicals

All chemicals were used as received. Products for synthesis are: 1,3-propanediol, PDO (DuPont Tate & Lyle), polytrimethylene ether glycol, PTEG ($\overline{M}_n$ = 634 g.mol-1, repeating PDO units = 10.6) (DuPont), sulfuric acid 96% RPE (Carlo Erba), sodium carbonate (Carlo Erba). Isosorbide (>99%) was a courtesy of Roquette (Lestrem). $CDCl_3$ (Euriso-top, 99,8%D), tetramethylsilane (Euriso-top) trifluoroacetic anhydride (TFAA) (Reagent-Plus, >99%, Sigma-Aldrich) were used for NMR analysis. Tetrahydrofuran HPLC grade Chromasolv® plus,>99.9% (Sigma-Aldrich) was used for Size Exclusion Chromatography. Methanol HiPerSolv Chromanorm (VWR Chemicals) was used for Solid Phase Extraction (SPE). Pyridine RS anhydrous for analysis (Carlo Erba), mixture of N,O-Bis(trimethylsilyl)trifluoroacetamide (BSTFA)–: trimethylchlorosilane (TMCS) 99 :1 (Supelco) were used for gas chromatography.

For the solubility tests and solid phase extraction purification, ultra-pure water (resistivity 18 MΩ.cm) was used.

Analytical methods

NMR spectra were recorded on Bruker Avance spectrometer at 400.13 MHz for ^{1}H and 100.61 MHz for ^{13}C with a 5 mm BBFO+ probe at 300K and processed with Bruker Topspin 3.2 software. All the samples were prepared in deuterated chloroform and derived by TFAA to distinguish the proton of the ethers (C***H₂***–O-C***H₂*** or isosorbide-O-C***H₂***) from the ends (C***H₂***-$OCOCF_3$). ^{1}H NMR, with ^{13}C GARP broadband decoupling for carbon satellites removal,[34] was used to determine ethers groups, end groups and free monomers. Chemical shifts are given in parts per million (ppm) and referenced to TMS as internal standard.

The Solid Phase Extraction (SPE) was used to remove free isosorbide from polymers. Cartridge was a Chromabond C18 2g (Macherey-Nagel). The solvents used were ultra pure water and methanol HiperSolv Chromanorm (VWR Chemicals). The sample was deposited on the cartridge and isosorbide was eluted by water. Then the copolymer was recovered by adding methanol. Methanol was evaporated under vacuum and the polymer fraction (P) recovered and ready for analysis and

characterization. Even if the copolymer is soluble in water, it is more retained on the silica than isosorbide. Then it is possible to separate isosorbide from every copolymer by this mean.

Thermal properties were obtained with a DSC Q20 equipped with a Liquid Nitrogen Cooling System (LNCS) (TA Instruments). Aluminum hermetic capsules were used and about 5mg sample were weighted. Samples were heated to +100°C, then cooled from +100°C to -130°C at a cooling rate of 10°C/min and heated from -130°C to 100°C at the same rate. Glass transition temperature (T_g) was determined during the cooling step and was taken at the mid-point. Crystallization and melting points were obtained from the second heating ramp and determined at the maximum of the peaks.

Thermogravimetric analyses are performed with a Q500 equipment (TA Instruments). Sample were weighted in aluminium pan then placed in an oven heated from ambient temperature to 600 °C at a rate of 10 °C/min. Nitrogen flow (90 ml/min) was introduced in the oven to avoid oxidations of the samples.

The MALDI-TOF mass spectrometry analysis was performed with a Voyager-DE PRO (Applied Biosystems, Framingham, MA) equipped with a nitrogen laser emitting at 337 nm with a 3 ns pulse duration. The instrument was operated in reflectron mode. The ions were accelerated under a potential of 20 kV. The positive ions were detected in all cases. The spectra were the sum of 300 shots and an external mass calibration of mass analyzer was used (a mixture of peptides, Sequazyme, Applied Biosystems, Framingham, MA). Samples were prepared by mixing 9 µL of 1,8,9-anthracenetriol (dithranol, purchased by Sigma-Aldrich) at 10 $g.L^{-1}$ in $CHCl_3$ with 10 µL of polymer 5 (at 10 $g.L^{-1}$ in $CHCl_3$). To enhance cationization of polymers, 1 µL of NaI (from Sigma-Aldrich, at 10 $g.L^{-1}$ in acetone) were added to solutions. Finally, resulting mixtures (1 µL) were spotted on the MALDI sample plate and air dried.

Typical procedure for the synthesis of polymers and etherification conditions

A first process (**process A**) of polymerization was inspired from literature.[23] A typical synthesis is described as follows: 1,3-propanediol (22.8 g, 0.3 mole) and isosorbide (43.8 g, 0.3 mole) were introduced into a four-neck round-bottom flask, stirred by a glass/Teflon® stirrer. Under nitrogen atmosphere the reactor was heated, with an electric heater, until the isosorbide melted. At this step, sulfuric acid was added (0.554g - 6.8 10^{-3} mole of catalyst/monomers). The reactants were heated to 150°C and water produced during reaction was removed thanks to nitrogen flow. Average number degree of polymerization of the whole sample excluding free isosorbide ($\overline{DP_n}$) were followed by ^{1}H NMR. After reaction, a solution of sodium carbonate (27 wt-%) was added into the reactor and the media heated at 95°C for 6h to hydrolyze ester sulfates. Final colored products were dehydrated under vacuum then filtrated. Free isosorbide content was determined by gas chromatography.

A second process (**process B**) was carried out by replacing PDO with PTEG-10.6 as a macrodiol monomer. PTEG-10.6 (24.0g, 0.0378 mole of PTEG) and isosorbide (58.45 g, 0.4 mole) were introduced into a four-neck round-bottom flask, stirred by a glass/Teflon® stirrer. Under nitrogen atmosphere the reactor was heated, with an electric heater, until the isosorbide melted. Same procedure was used as above with 0.56g - 6.85 10^{-3} mole of sulfuric acid/monomer unit. The reactants were heated to 150°C and water produced during reaction was removed thanks to nitrogen flow. Average number degree of polymerization ($\overline{DP_n}$) and monomers conversion content were followed by ^{1}H NMR. After reaction, a solution of sodium carbonate (27 wt-%) was added into the reactor and the media heated at 95°C for 6h to hydrolyze ester sulfates. Final colored products were dehydrated under vacuum then filtrated. Free isosorbide content was determined by gas chromatography.

Computational details

All the calculations were performed at the DFT level using the Gaussian 09 package.[35] The B3LYP[36,37] hybrid functional and the 6-31g(d,p) double zeta and polarization basis set[38,39] were chosen.

In order to have a more realistic description of the system, the calculations were performed in presence of solvent. The solvent was described with the SMD model, as implemented in Gaussian 09.[40] A different choice of the solvent was made for the two processes. In particular, both a diol and an ether were considered, in order to reproduce the two different reaction environments; among the solvent implemented in Gaussian, the 1,2-ethane-diol and the diethyl ether were chosen. The thermodynamic quantities were evaluated at the experimental reaction temperature of 150 °C.

3 Results and discussion

3.1 Preparation and characterization of PDO-isosorbide copolymers

The copolyetherification reaction involving 1,3-propanediol (PDO) and isosorbide (ISO) (**process A**) is supposed to lead a copolymer with statistic microstructure according to the chemical scheme reported Figure 2. A first trial with an ISO/PDO molar ratio of 20/80 was performed over a period of 14 hours and in the presence of H_2SO_4 as catalyst. To perform ^{1}H NMR analysis, the crude product (copoA1, Table 2) was first solubilized in 0.7 ml of $CDCl_3$ containing 200 µl of trifluoroacetic anhydride (TFAA) in order to cap the hydroxyl group at the extremity and thus avoid hydrogen interactions leading to more complex NMR signals. NMR Spectra (Figure 4) highlights the two characteristic signals of the PTEG blocks at 1.94 ppm and 3.62 ppm and the three specific signals at 2.06, 4.47 and 4.73 ppm belonging to the hydrogen of PDO units at the extremities of copolymer chains. The signals of isosorbide units are also detected between 4.51 and 5.39 ppm (Figure 4). All these data prove the presence of the different units but failed to prove that isosorbide units are linked to the one of PDO. Though considering the ^{13}C chemical shifts of different isosorbide ethers available in the literature, it was possible to propose an attribution for the protons chemical shift through a two dimension ^{1}H-^{13}C HSQC experiment.[25,29,41] These results (SI Figure 2) allow the correlation between carbon C_3 and C_4 of isosorbide and corresponding H_3 and H_4 respectively and highlight that three new signals consistent to new derivatives are present next to the protons H_3 and H_4 of isosorbide. In addition those data and another ^{1}H COSY features (SI Figure 3) reveal two different zones for carbons C_2 and C_5: between 77 and 82 ppm corresponding to the carbons linked to the trifluoro acetic acid group and between 80.4 and 84 ppm for those directly linked to PDO units. Finally, a ^{1}H-^{13}C HMBC (Heteronuclear Multiple Bond Correlation) experiment confirms the ligation of the isosorbide units to PDO unit (SI Figure 4) giving the possibility to propose the different sub-structures existing in the crude product (Figure 3) and their attribution (Table 1).

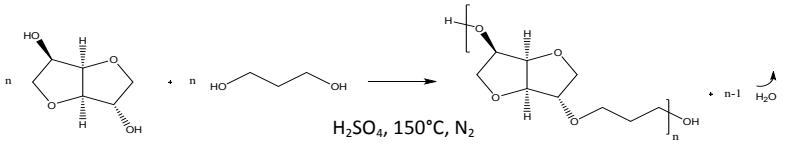

Figure 2: Etherification reaction between isosorbide and 1,3-propanediol, in acidic conditions.

NMR data also permit the quantitative determination of i/ the isosorbide conversion, ii/ the $\overline{DP}_n$, iii/ the molar mass $\overline{M}_n$, iv/ the molar percentage of the isosorbide diether in polymer chains, v/ the percentage of isosorbide end units based on the total ends chains of copolymer and their substitution: 5*O* or 2*O* isosorbide ether end chain and vi/ the percentage of free isosorbide (see SI Eq. 11 for the calculation).

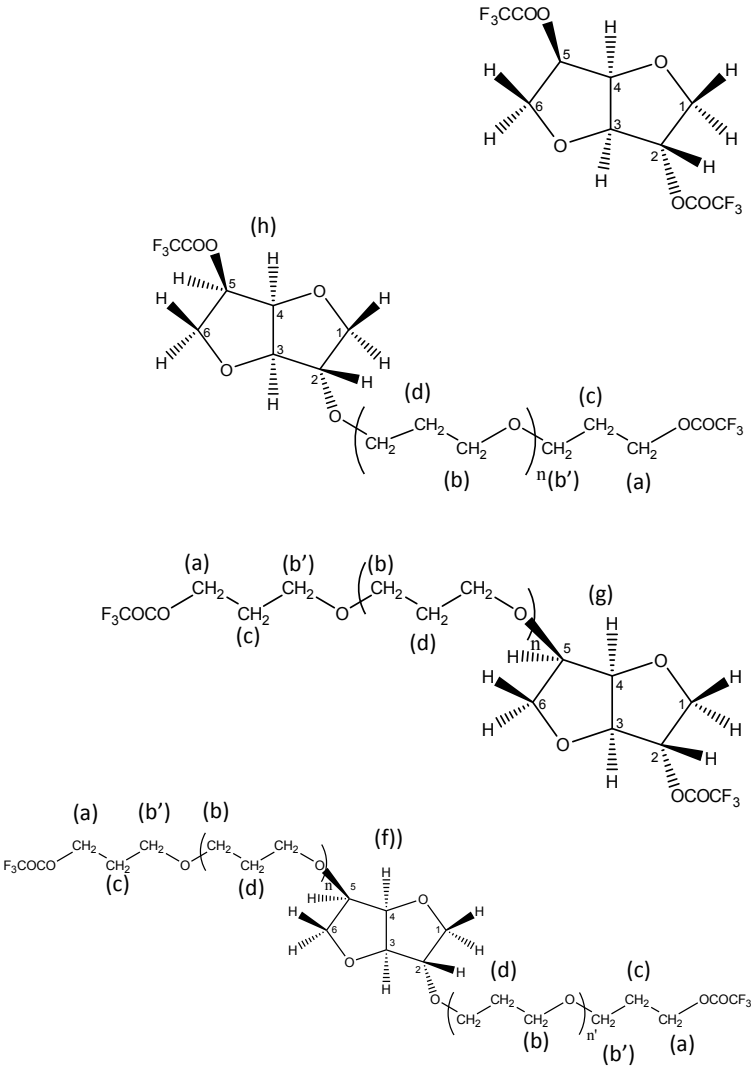

(I) Isosorbide ditrifluoroacetate

Corresponding to H_{2iso}; H_{3iso}; H_{4iso}; H_{5iso} on figure 4.

(II) 2O-PTEG-isosorbide monoether ditrifluoroacetate

Corresponding to H_2-2O; H_3-2O; H_4-2O on figure 4.

(III) 5O-PTEG-isosorbide monoether ditrifluoroacetate

Corresponding to H_3-5O; H_4-5O; H_5-5O on figure 4.

(IV) 2O-5O-PTEG-isosorbide diether ditrifluoroacetate

Corresponding to H_3-2O-5O; H_4-2O-5O on figure 4.

Figure 3: Structures of isosorbide ethers and free isosorbide present in the copoA1, **process A**, derivatized with trifluoroacetic anhydride (TFAA). (I) Isosorbide ditrifluoroacetate, (II) 2O-PTEG-isosorbide monoether ditrifluoroacetate, (III) 5O-PTEG-isosorbide monoether ditrifluoroacetate, (IV) 2O-5O-PTEG-isosorbide diether ditrifluoroacetate.

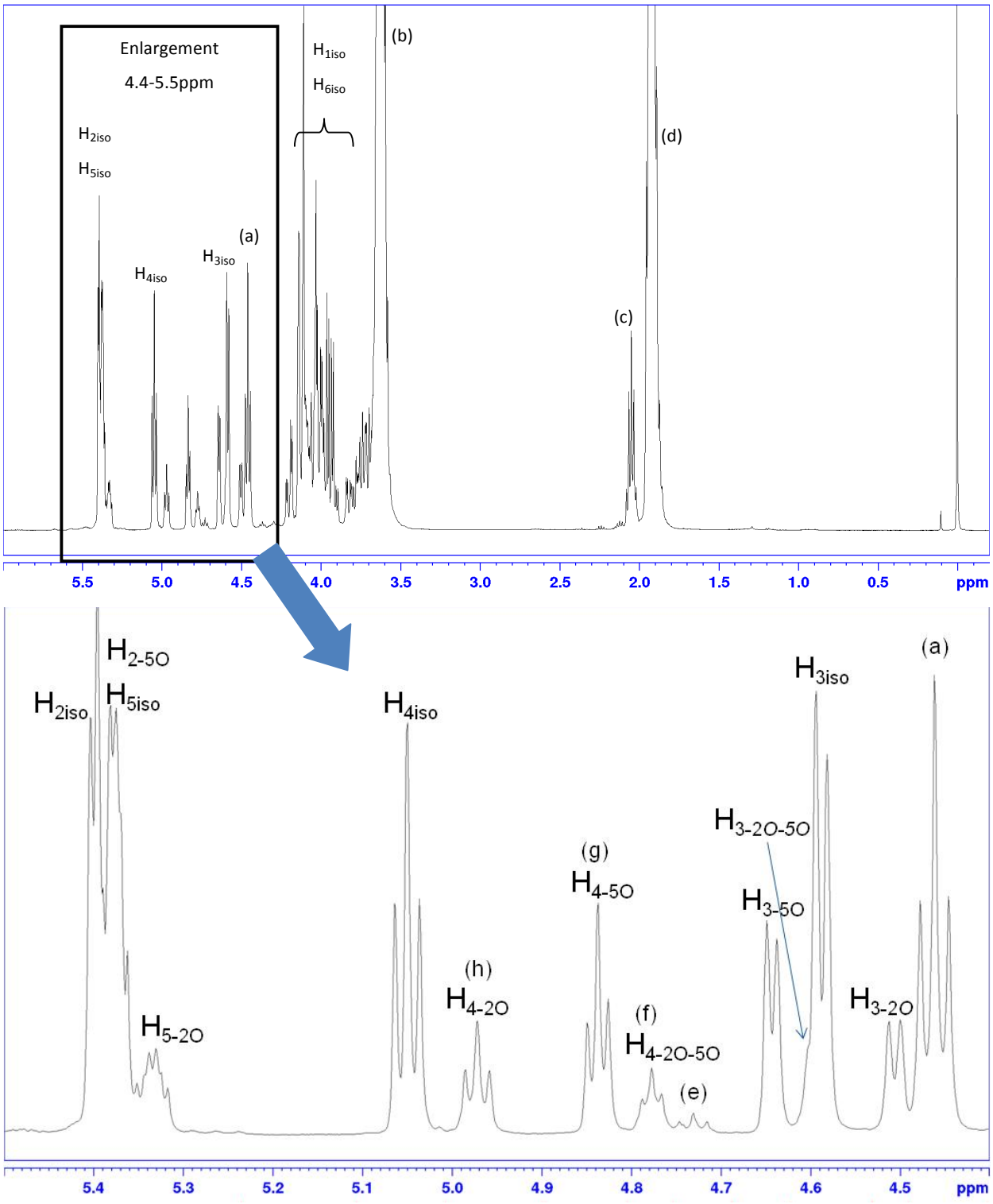

Solvent $CDCl_3$; T=300K

Figure 4: ^1H NMR spectra of PDO-isosorbide copolymer (copoA1, process A), derivatized with trifluoroacetic anhydride (TFAA), $CDCl_3$, 300K

Chemical shift (ppm)	Corresponding signal	Proton numbering (Figure 3 and Figure 4)
1.94	-O-(CH_2-C***H₂***-CH_2-O)$_n$- (main chain)	d
2.06	-O-CH_2-C***H₂***-CH_2-O-$COCF_3$ (chain end)	c
3.62	-O-(C***H₂***-CH_2-C***H₂***-O)$_n$- (main + chain end)	b
4.47	-O-CH_2-CH_2-C***H₂***-O-$COCF_3$	a
4.73	-C***H₂***-OSO_3-$COCF_3$ (chain end)	e
4.78	Isosorbide H_4 2*O*-5*O* isosorbide diether (unit)	f
4.84	Isosorbide H_4 5*O* isosorbide monoether in C_5 (chain end)	g
4.98	Isosorbide H_4 2*O* isosorbide monoether in C_2 (chain end)	h
5.05	Isosorbide	H_{4iso}

Table 1 : chemical shift of the protons in copolymer PDO-isosorbide ($CDCl_3$ + TFAA)

3.2 Influence of the process parameters on the final copolyethers structures

For copoA1 one can observe that the conversion of isosorbide is limited to 49 mol % after 14 hours of reaction and as a consequence that the molar mass is limited to a low level ($\overline{M}_n$ = 875 g.mol^{-1}). More surprisingly data suggest that the isosorbide moieties are mainly located at the extremity of the polymer chain (59.6% mol % of isosorbide ends) and that the isosorbide diether unit inside the polymer backbone remains low (2 mol %) (Table 2).

In order to increase the isosorbide content within the polymer, the molar ratio ISO/PDO was set to 50/50 (copoA2) in the initial reaction medium. Both molar mass and isosorbide conversion were followed as a function of time and the results are reported in Figure 6. An increase of the conversion of isosorbide and of the molar mass was observed reaching a plateau after 12 hours of reaction. The final molar mass was $\overline{M}_n$ = 600g.mol^{-1}, which is lower than for copoA1. The isosorbide conversion was higher (64 mol % instead of 49 mol %) with also an increase of the isosorbide units inside polymer chain (39 mol %). More remarkably the analysis revealed that the chain extremities were constituted almost exclusively with isosorbide units (94% mole). The latter result was also supported through MALDI-TOF mass spectrometry analysis (SI Figure 5) where three populations (population 1, 2 and 3) of PDO-isosorbide oligomers are clearly evidenced. Thus Figure 5 shows an enlargement of the mass spectrum where the first population at 819.5 m/z can match a molecular formula of [$C_{39}H_{72}O_{16}$ + Na]$^+$ which corresponds to a structure containing two isosorbide end-groups and nine PDO units (population 1, n=9). The one at 831.5 m/z is attributed to [$C_{39}H_{68}O_{17}$ + Na]$^+$, corresponding to a structure constituted of one isosorbide unit within the chain, seven PDO units distributed on either side of the intra-chain isosorbide unit and two isosorbide end-groups (population 2, x+x'=7). Finally, the signal at 843.5 m/z is ascribed to the molecular formula[$C_{39}H_{64}O_{18}$ + Na]$^+$, corresponding to a structure containing two isosorbide units in the chain, five PDO units distributed on either side of the isosorbide units and two isosorbide end-groups (population 3, y+y'+y''=5).

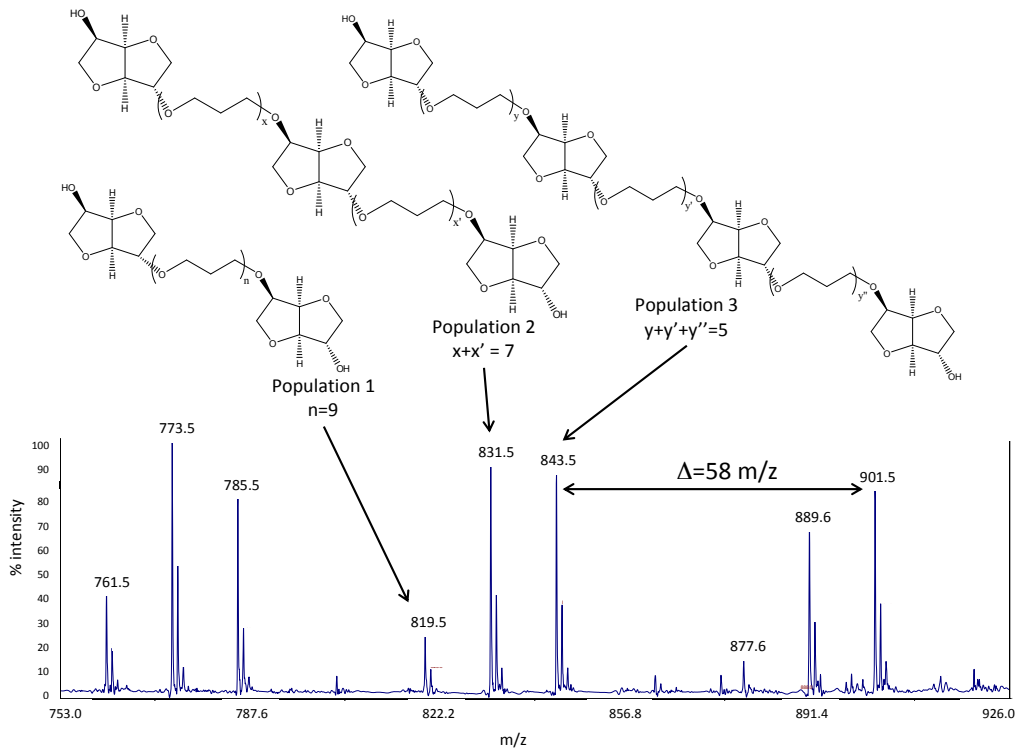

Figure 5: enlargement of positive ion MALDI-TOF mass spectrum of copoA2 (dithranol matrix, NaI salt, reflectron mode).

Another trial with the same reagent ratio but at higher temperature: 167°C (copoA3) gave also a high quantity of isosorbide end-chains. Moreover slightly lower isosorbide conversion was measured probably due to isosorbide degradation during time.

Trials were also performed with **process B** where the PDO is replaced by a PTEG As for the **process A**, trials were performed at high temperature and in the presence of H_2SO_4. The increase of ISO/PDO initial molar ratio (16/84, 36/64, 50/50 and 69/31 for respectively copoB1, copoB2, copoB3 and copoB4) clearly induced the overall conversion of the isosorbide and favored its presence at the extremity. It is also interesting to point out that the molar mass decreases when the initial isosorbide content increases (Figure 7), indicating that isosorbide could play the role of an end-capped agent and that transetherification is occuring.

The **process B** has also an impact on the structure of the copolyether, especially on the isosorbide diether content, even if the molar ratio between isosorbide and PDO units is equal. Starting with the same molar ratio isosorbide / PDO units (50/50), the **process A** gave higher isosorbide diether content (11.7 mol %; copoA2) than the **process B** which involves PTEG-10.6 (2.2 mol % of isosorbide diether, copoB3). The OH reactive ends of the PDO are more numerous to etherify isosorbide than the OH chain ends of PTEG-10.6. Using data from Table 2, the structure of copoB3 can be described as PTEG block of six PDO unit with one isosorbide unit on each end, whereas the chains of copoA2 are constituted by mean with four PDO (x+x'=4) units distributed on both sides of an isosorbide unit then terminated by one isosorbide unit on each chain end (see structure of population 2, Figure 5).

Sample	Process conditions				General polymer chains characteristics[a]				Content of the different structures of isosorbide in the polymer chains (mole %)		
	Diol 1 mole	Diol 2 mole	Iso. /PDO (molar ratio)	Time (h)	$\overline{DP_n}$	$\overline{M_n}$ g.mol^{-1}	Iso. /PDO (molar ratio)	Free isosorbide % by weight	Iso diether / total units	Iso.diether / iso. in polymer	Terminal iso / total ends
copoA1	Isosorbide 0.12	PDO 0.48	20/80	14	13.2	875	11/89	18.2	2.0	18.2	59.6
copoA2	Isosorbide 0.3	PDO 0.3	50/50	21	6.9	610	39/61	20.7	11.7	30.2	94.4
copoA3	Isosorbide 0.3	PDO 0.3	50/50	21	6.8	580	36/64	23.5	8.9	24.6	91.9
copoB1	Isosorbide 0.3	PTEG-10.6 0.15	16/84	12	18.6	1183	7/93	14.9	0.0	0	60.6
copoB2	Isosorbide 0.3	PTEG-10.6 0.05	36/64	12	9.7	720	20/80	29.5	3.8	18.4	81.2
copoB3	Isosorbide 0.4	PTEG-10.6 0.0377	50/50	6	7.6	582	24/76	46.9	2.2	9.3	81.0
copoB4	Isosorbide 0.46	PTEG-10.6 0.022	69/31	12	4.9	455	45/55	48.2	5.6	12.5	93.5
Homo1	Isosorbide 0.5	-	100	6	1.0	No dimer nor oligomer detected			-	-	-
Homo2	PDO 33	-	0	25	21.6	1360	-		-	-	-

(a) Calculation details, see SI Eq.1 to Eq.11.

Table 2: Experimental conditions for synthesis of homopolymers (homo1 and homo2) and PDO- isosorbide (iso.) copolymers. H_2SO_4 concentration = $6.8.10^{-3}$ mol./mol. of PDO and isosorbide units except copoB2: $2.8.10^{-3}$; T=150°C except copoA3 and Homo2: T=167°C. Polymers structures determined by ^{1}H NMR, $\overline{DPn}$, % isosorbide and diether isosorbide units in the polymer chain, percentage of isosorbide chain ends, free isosorbide. No free PDO is observed.

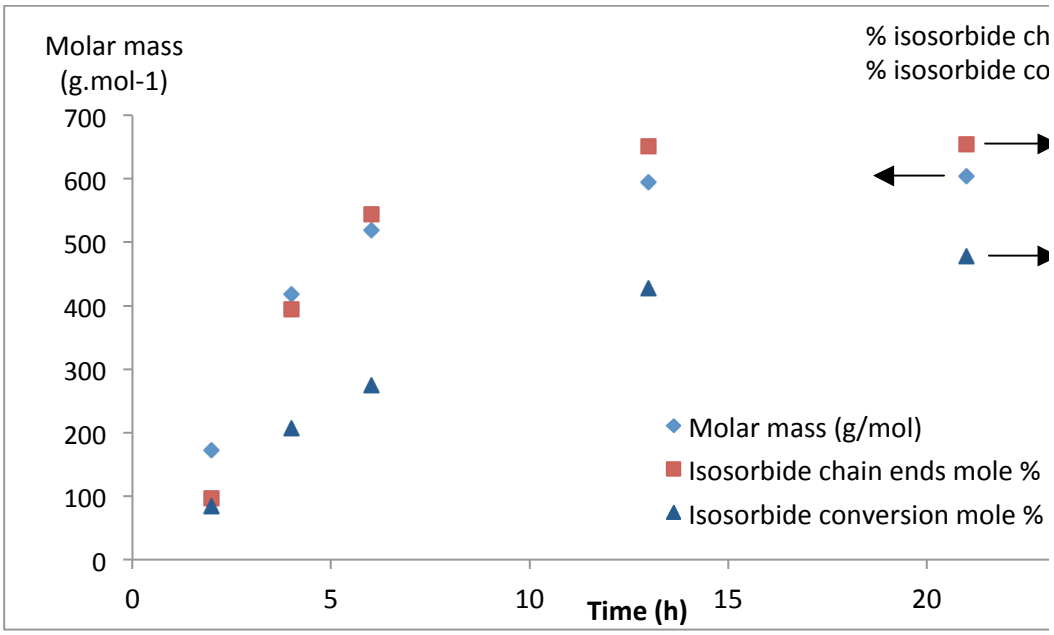

Figure 6: Evolution of molar mass oligoethers chains $\overline{M}_n$ and % of isosorbide in chain ends during polycond and isosorbide (molar ratio 50:50) (copoA2)

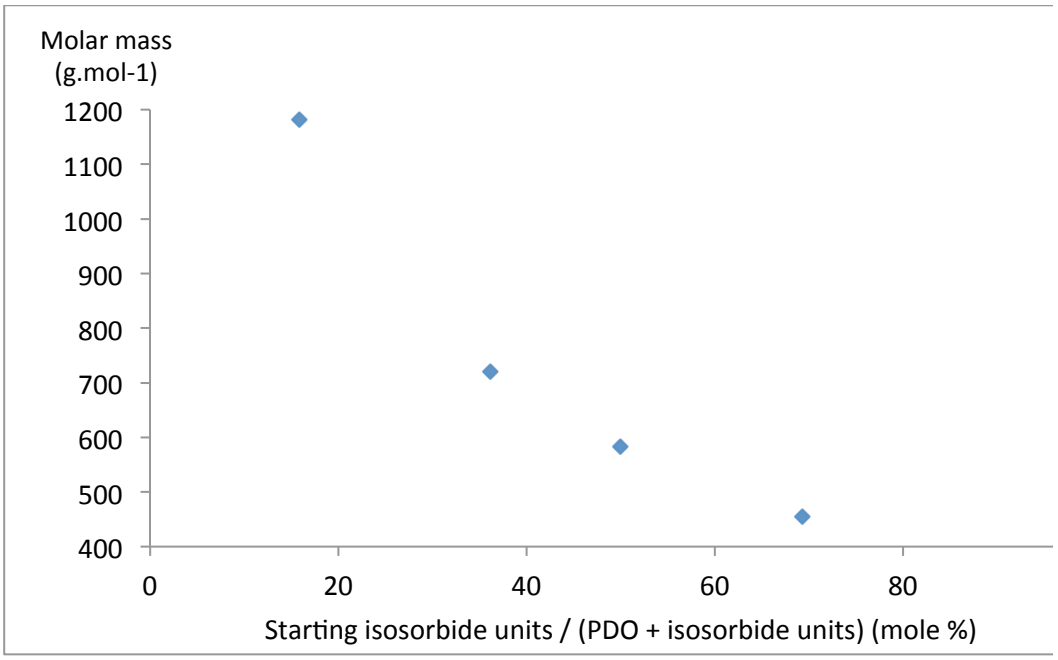

Figure 7: Molar mass of PDO-isosorbide copolymer ($\overline{M}_n$), depending of initial isosorbide content follc (150°C and 6.85 10^{-3} mole of sulfuric acid/monomer unit).

Whatever the process, **process A or process B**, the molar masses of the resulting products are low ma presence of isosorbide units at the polymer chain-ends and the fact that isosorbide monomer did not react no dimer units were evidenced by the NMR analysis of co-oligomers described above. In addition the etheri with only isosorbide monomers was unsuccessful (see trial homo1 on Table 2).

Computational calculations were performed to confirm the previous results. First the calculation of ΔG for the dimerization of the isosorbide, at 150°C and in 1,2-ethanediol, gave positive values, from +12 to +27 $kJ.mol^{-1}$, depending of the considered dimer (hypothetical dimerization of the isosorbide could give three different structural isomers - Figure 1a). These results highlight the fact that the formation of possible dimers and presumably higher oligomers of isosorbide is unfavorable, in agreement with the absence of any isosorbide homopolymer noted experimentally.

Once excluded the possible dimerization of the isosorbide, the etherification reactions possible in the **process A** are: i/ the dimerization of the PDO and ii/ the reaction of PDO with isosorbide through reaction of hydroxyl in C2 and C5 position. The calculated Gibbs free energies of formation are summarized in Table 3. The results show that, among the three reactions, the dimerization of the PDO and the reactions of the PDO with the isosorbide on C2 have a similar reaction free energy considering the margin of errors in the methods and are the most favorable ones on a thermodynamic basis. However, the reaction of PDO with the isosorbide on C5 is only ~10 $kJ.mol^{-1}$ more endergonic.

Product	ΔG of formation ($kJ.mol^{-1}$)
PDO-isosorbide-C2	+3
PDO-isosorbide-C5	+12
PDO-dimer	-1

Table 3: Calculated values for ΔG of ether formation.

When the process involves a chain longer than one PDO, five different reactions with the isosorbide are possible (Figure 8). The reactions I, II represent the etherification reactions, with the release of one molecule of water, while the reactions IV and V are transetherification resulting in the breaking of the polymeric chain. Reaction III involves both etherification and transetherification reactions.

We also have considered the formation of the 4-PDO unit's oligomers formation starting from two PDO-dimers. This oligomer can be in two conformations: bent or linear. As the Gibbs free energy is +3 kJ.mol-1 for the bent form and 11 $kJ.mol^{-1}$ for the linear, the bent form is preferred for the rest of the computational simulation.

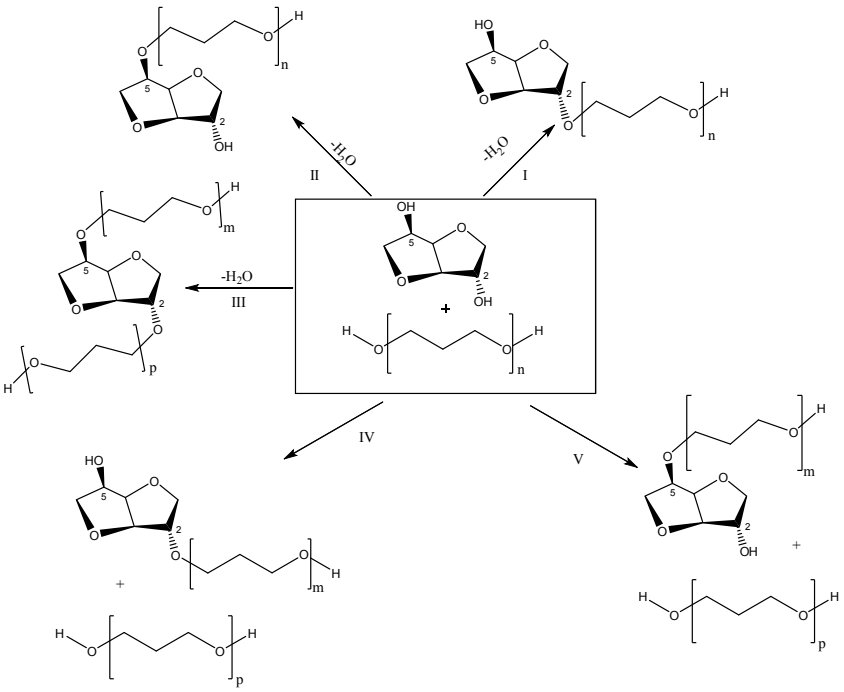

	ΔG of formation (kJ.mol^{-1})
Path	4 units PDO bent
I (C2)	11
II (C5)	17
III	24
IV (C2)	2
V (C5)	13
	Formation of 4 units PDO
Bent	3

Figure 8: Scheme of possible reactions between isosorbide and PTEG (represented by a dimer of PDO) in the 1,2-ethanediol at 150° C. ΔG of formation of the five processes are given on a side table (The C of the isosorbide involved in the process is specified in parenthesis).

The thermodynamic of these reactions was studied using 4 PDO units oligomer in the bent form, with 1,2-ethanediol as solvent and at 150°C. The formation of the 4-units polymer starting from two dimers was also taken into account. For each path presented in the Figure 8, the calculated Gibbs free energy, expressed in KJ.mol-1, is summarized on side table. The results show that the Gibbs free energies of the transetherification reaction (path IV for C2 and path V C5) are lower than the etherification path for the same carbon involved (path I for C2 and path II for C5). That means that the transetherification reactions are slightly favored with respect the etherification, regardless of the nucleophilic group of the isosorbide involved in the reaction. The differences in energy, however, suggest that the etherification and transetherification are competitive. The path III, involving an etherification and a transetherification, bringing to a double etherification of the isosorbide, is the highest energy process. This is in agreement with the experiments, according to whom only a few percentage of "inner" isosorbide is detected. By combining the experimental and computational results, one can draw the different pathways involving etherification and/or transetherification during the two copolyetherification **processes A and B** (Figure 9).

Numerous studies highlighted that the reactivity of the hydroxyl groups of isosorbide molecule is influenced by the steric hindrance, but also by the reagent and reaction medium used. As example, acetylation of isosorbide by acetic anhydride in presence of scandium(III) triflate conduct to a ratio of 4:1 between *endo*-acetate and exo-acetate[42]. Acetylation by acetic anhydride in pyridine favors the 2 position and in contrary pyridine hydrochloride promotes acylation at position 5[43]. The conditions that enhance activation of endo-5-hydroxyl group or stabilize by solvation the position 2 favor the 5-acetalyted products. Unfortunately the reactions conditions, prior to experimental, do not allow prediction of the reaction pathway[44].

Herein the more initial isosorbide is introduced, the more isosorbide di-ended species are formed. In addition, the ratio between monoether C5 (5O) and monoether C2 (2O) remained constant at 60/40 for **processes A** and **B**, indicating that the reactivity of hydroxyl functions on C2 and C5 are close but not strictly equivalent. Finally the isosorbide plays the role of an end-capper reagent giving rise a telechelic structure.

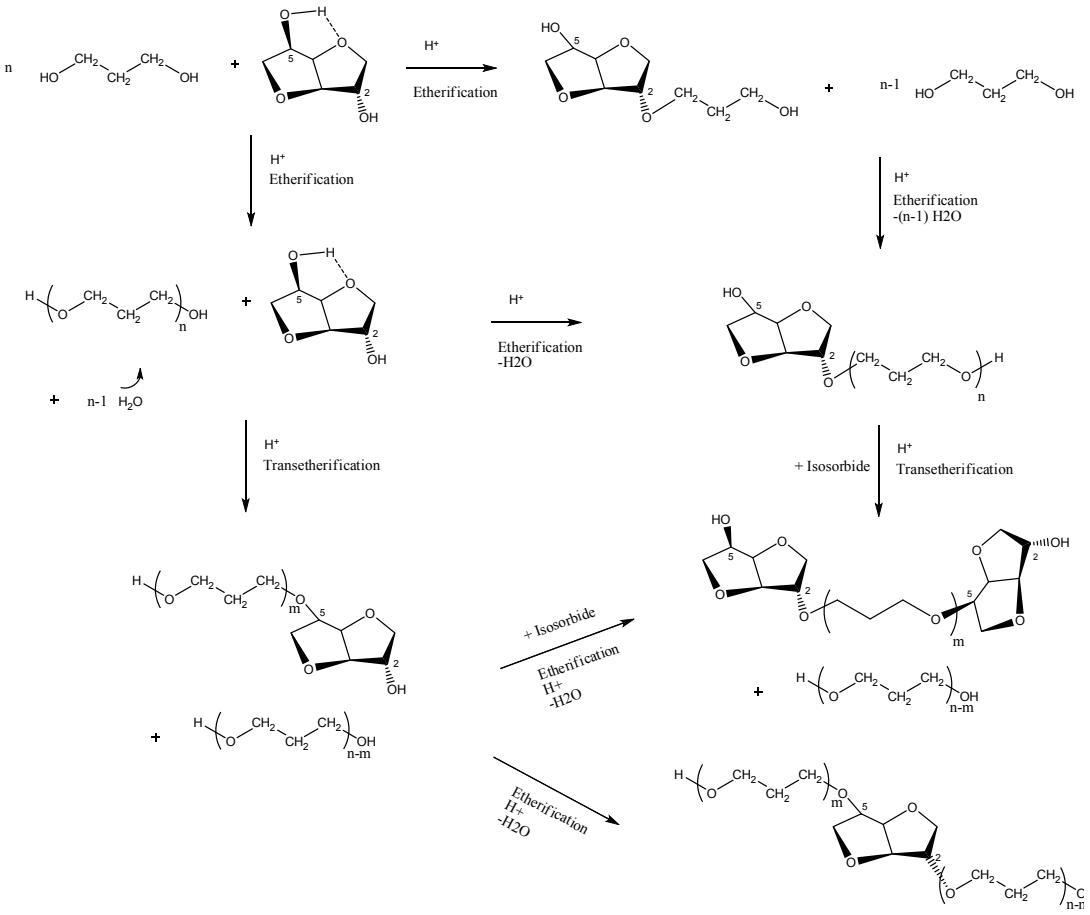

Figure 9: Reactions occurring during PDO-isosorbide polymerization or transetherification of PTEG by isosorbide.

3.3 Properties of copolyethers of 1.3-propanediol-isosorbide

The thermal properties of copolymers were evaluated both with neat samples, copoA2, copoA3 and copoB3 and with purified samples, copoA1 P, copoA2 P, copoB3 P, in which the free isosorbide has been removed by SPE. All of them were compared with properties of PTEG having equivalent molar masses. First whatever the composition and the molar mass of copolymers neither exotherm nor endotherm was detected meaning that the copolymers are amorphous. This feature highlights the role of the isosorbide units onto the properties of the backbone, the homopolymer of PDO with $\overline{M'}_n$ of 630 g.mol^{-1} giving a crystallization exotherm at -37°C and two melting endotherms at 0 and 9°C. In addition it is interesting to point out that the physical blend of isosorbide and PTEG are also crystalline indicating that only internal isosorbide ether may hamper unit the crystallization. In contrast the T_g is impacted both by the presence of free isosorbide molecule and isosorbide ether unit. Thus for sample copoA2, copoA3 and copoB3 the Tg are 41°C, 47°C, 57°C respectively whereas for purified samples copoA2 P, copoA3 P, copoB3 P and copoA1 P the T_g are -34, -33, -53°C and -62°C for a molar content of isosorbide of 39.5 , 36.8, 23.9 and 11.0 mol-% respectively.

Thus T_g values of copolymers are higher than the T_g of the PDO homopolymers having a similar molar mass, the introduction of the two-fused tetrahydrofuran rings increasing the stiffness of the copolymer as also shown with other copolymers such as copolyesters or polyurethanes.[27,45]

Sample	Iso/PDO Molar ratio	M_n g.mol^{-1}	T_g (°C)	$T_{d(5\%)}$ (°C)	% Residual Mass	Water solution aspect at 1 wt-%		
						At 20°C	At 40°C	At 60°C
CopoA1 P	11/89	875	-62	260	0.4	nd	nd	nd
CopoA2	50/50	370	-41	217	3.2	soluble	soluble	soluble
CopoA2 P	39/61	600	-34	280	4.4	nd	nd	nd
CopoB3	50/50	240	-57	154	1.1	soluble	slightly soluble	insoluble
CopoB3 P	24/76	580	-53	257	2.7	nd	nd	nd
Homo3	0/100	230	-95	N.D.	N.D	soluble	soluble	soluble
Homo 4	0/100	630	-85	177	0.4	insoluble	insoluble	insoluble
Homo 4 + Free Isorbide	28/72	630	nd	nd	nd	insoluble	insoluble	insoluble

nd: non determined

Table 4: physical properties of isosobide-PDO copolymers and PDO homopolymers.

The thermal stability of oligoethers was also investigated by means of thermogravimetric analysis. Three oligomers having equivalent molar mass but different compositions: copoA2 P ($\overline{M'}_n$ = 610 g.mol^{-1}, 94 mole % isosorbide ends), copoB3 P ($\overline{M'}_n$ = 580 g.mol^{-1}, 81 mole % isosorbide ends) and Homo4 ($\overline{M'}_n$ = 630 g.mol^{-1}), were compared. The thermograms gathered Figure 10 clearly evidence that the degradation temperature when the masses loss is 5% ($Temp_{5\%}$) for copoA2 P and copoB3 P is 280 and 257 °C respectively and is thus 80°C higher than the $Temp_{5\%}$ of the homo4 (177 °C). This trend is also confirmed if one considers the onset and offset temperature values and is valuable for samples with higher molecular weight but lower isosorbide content (CopoA1 P). Thus these results illustrate the impact of the isosorbide ether units and particularly the ones located at the chain extremities. Indeed the oligomers copoA2 P shows the best thermal stability.

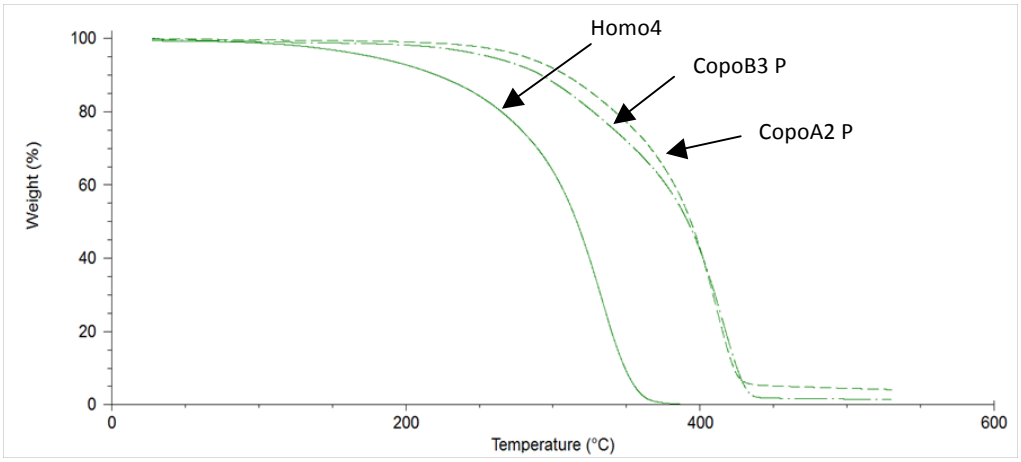

Figure 10: Thermograms TGA of homo4, copoA2 P and copoB3 P (under N_2)

The incorporation of Isosorbide moiety being favorable for increasing the hydrophilicity as already shown in the literature for the preparation of hydrotropes [24,25,46], an increase of the water solubility of the oligomers having isosorbide ether units was expected. This feature was characterized with non-purified compounds: CopoA2, copoB3, homo3 and homo4, the purification method not allowing the preparation of enough quantity of product for the solubility tests. Thus the co-oligomer tested contained free isosorbide. The results given innd: non determined

Table 4 highlight that the PTEG homopolymer having the lowest molar mass (homo3 ; $\overline{M'}_n$ of 230 g.mol^{-1}) is water soluble at room temperature whereas the one with higher molar mass (homo4 ; $\overline{M'}_n$ of 630 g.mol^{-1}) remains insoluble. In addition the introduction of free isosorbide into a dispersion of homo4 in water gave rise no amelioration, the homo4 being always non soluble. Conversely the oligomers bearing isosorbide ether units are water soluble. More precisely the CopoA2 is soluble whatever the temperature: 25, 40 and 60°C whereas copoB3 containing less isosorbide ether units is water soluble at 25°C but partially soluble at 40°C and non-soluble at 60°C. This features meet the behavior of certain alcohol ethoxylates, exhibiting a cloud point temperature discussed in detail by Rupert.[47]

4 Conclusion

Novel copolyethers based on 1,3-propanediol and isosorbide were prepared according to two different processes: co-etherification of PDO and isosorbide (process A) and transetherifcation of isosorbide and PTEG (process B), both in acidic conditions at 150°C. The structural characterization of copolyethers by means of complementary analysis methods: 2D and ^{1}H NMR, gas chromatography analysis, coupled with FID and MS-MALDI-TOF mass spectrometry have shown that the final structures of the copolymers greatly depend on the initial isosorbide/PDO molar ratio. Data also allow proposing two mechanisms involving during the reaction: etherification and trans-etherification where isosorbide reacts decreasing the molar mass through segmentation of polymers chains. Both mechanisms take place in process A and B but not at the same level and as a consequence the final structures are similar but not completely identical. In particular the concentration of inner isosorbide units is different. Another important feature is that the low reactivity of isosorbide hydroxyl gives at the end of the reaction a telechelic polymer structure with isosorbide units located at each chain extremity. In parallel a computational calculations have well duplicated the experimental results. Finally evaluation of thermal and solubility properties confirms the expected great interest of isosorbide units which bring higher compatibility to water and higher T_g level and thermal stability. Thus one can envisaged to engage this novel and original bio-based copolyether as reactive macrodiol in various reactions and systems opening new opportunities for the design of bio-based materials.

Acknowlegments

Authors thank Gattefossé SAS for the financial support and Roquette for providing the isosorbide. The help of Catherine Ladavière for the MALDI-TOF mass spectrometry analysis is also acknowledged as well as the help of Fernande Boisson for the NMR analysis.

References

1. J.J. Bozell, G.R. Petersen. *Green Chem.*, 2010, **12**, 539.

2. A. Behr, J. Eilting, K. Irawadi, J. Leschinski, F. Lindner. *Green Chem.*, 2008, **10**, 13.

3. E. Celinska. *Biotechnol. Adv.*, 2010, **28**, 519.

4. T. Haas, B. Jaeger, R. Weber, S.F. Mitchell, C.F. King. *Appl. Catal. , A*, 2004, **280**, 83.

5. G. Kaur, A.K. Srivastava, S. Chand. *Biochem. Eng. J.*, 2012, **64**, 106.

6. R.K. Saxena, P. Anand, S. Saran, J. Isar. *Biotechnol. Adv.*, 2009, **27**, 895.

7. R.C. Morris, A.V. Snider. Patent FR952490. 17 November 1949. (N. V. De Bataafsche Petroleum Maatschappij)

8. R. Mason. Patent US3326985A. 20 June 1967. (Shell)

9. A.W. Etchells, F. Godbille, H. Liang, H.B. Sunkara. Patent WO2011057236A2. 12 May 2011. (DuPont)

10. M.A. Harmer, D.C. Confer, C.K. Hoffman, S.C. Jackson, A.Y. Liauw, A.R. Minter, E.R. Murphy, R.E. Spence, H.B. Sunkara. *Green Chem.*, 2010, **12**, 1410.

11. H.B. Sunkara. Patent US2008175875A1. 24 July 2008. (DuPont)

12. H.B. Sunkara, R. Poladi, R. Prasad. Patent WO2009048445A2. 9 April 2009. (DuPont)

13. H.B. Sunkara. Patent US8029812B2. 4 October 2011. (DuPont)

14. H.B. Sunkara. Patent US20060192173A1. 31 August 2006. (DuPont)

15. A. Yokoyama, H. Sunkara, R. Saliya. *Eur. Coat. J.*, 2012, 26.

16. H.B. Sunkara, R. Poladi, G. Fenyvesi. Patent US20080108845. 8 May 2008. (DuPont)

17. Sunkara,H.B. Renewably sourced high performance poly(trimethylene ether) polyols for CASE applications. In : PMSE Prepr., 2012, ISBN 1550-6703.

18. P.A. Mueller, E.R. Murphy, B. Rajagopalan, J.P. Congalidis, A.R. Minter. *Macromolecular Symposia*, 2011, **302**, 56.

19. W.J. Cui, K.B. McAuley, R.A. Whitney, R.E. Spence, T. Xie. *Macromol. React. Eng.*, 2013, **7**, 237.

20. P.A. Mueller, B. Rajagopalan, J.P. Congalidis, E.R. Murphy. *Macromol. React. Eng.*, 2012, **6**, 126.

21. W.J. Cui, K.B. McAuley, R.E. Spence, T. Xie. *Macromol. React. Eng.*, 2014, **8**, 476.

22. H.N. Lee, B.M. Rosen, G. Fenyvesi, H.B. Sunkara. *J. Polym. Sci. , Part A: Polym. Chem.*, 2012, **50**, 4311.

23. H.B. Sunkara, H.Q. Do. Patent US7244810. 12 February 2004. (DuPont)

24. G. Fleche, M. Huchette. *Starch/Staerke*, 1986, **38**, 26.

25. Y. Zhu, V. Molinier, M. Durand, A. Lavergne, J.-M. Aubry. *Langmuir*, 2009, **25**, 13419.

26. F.J. Hopton, G.H.S. Thomas. *Can. J. Chem.*, 1969, **47**, 2395.

27. F. Fenouillot, A. Rousseau, G. Colomines, R. Saint-Loup, J.P. Pascault. *Prog. Polym. Sci.*, 2010, **35**, 578.

28. R. Muelhaupt. *Macromol. Chem. Phys.*, 2013, **214**, 159.

29. Y. Zhu, M. Durand, V. Molinier, J.-M. Aubry. *Green Chem.*, 2008, **10**, 532.

30. J.G. Morrison. Patent US3041300. 26 June 1962. (Martin Marietta Corp)

31. S. Chatti, M. Bortolussi, A. Loupy, J.C. Blais, D. Bogdal, M. Majdoub. *Eur. Polym. J.*, 2002, **38**, 1851.

32. S. Chatti, M. Bortolussi, D. Bogdal, J.C. Blais, A. Loupy. *Eur. Polym. J.*, 2004, **40**, 561.

33. R. Medimagh, S. Chatti, S. Alves, N. Hammed, A. Loupy, H. Zarrouk. *C. R. Chim.*, 2007, **10**, 234.

34. G.F. Pauli, B.U. Jaki, D.C. Lankin. *J. Nat. Prod.*, 2007, **70**, 589.

35. Gaussian 09, Edition D.01. Gaussian Inc., Wallingford CT, 2009.

36. A.D. Becke. *J. Chem. Phys.*, 1993, **98**, 5648.

37. P.J. Stephens, F.J. Devlin, C.F. Chabalowski, M.J. Frisch. *J. Phys. Chem.*, 1994, **98**, 11623.

38. G.A. Petersson, A. Bennett, T.G. Tensfeldt, M.A. Al-Laham, W.A. Shirley, J. Mantzaris. *J. Chem. Phys.*, 1988, **89**, 2193.

39. G.A. Petersson, T.G. Tensfeldt, J.A. Montgomery. *J. Chem. Phys.*, 1991, **94**, 6091.

40. A.V. Marenich, C.J. Cramer, D.G. Truhlar. *J. Phys. Chem. B*, 2009, **113**, 6378.

41. A. Lavergne, Y. Zhu, V. Molinier, J.-M. Aubry. *Colloids Surf. , A*, 2012, **404**, 56.

42. J.J. Gallagher, M.A. Hillmyer, T.M. Reineke. *ACS Sustainable Chem. Eng.*, 2015, **3**, 662.

43. K.W. Buck, J.M. Duxbury, A.B. Foster, A.R. Perry, J.M. Webber. *Carbohydr. Res.*, 1966, **2**, 122.

44. P. Stoss, R. Hemmer. *Adv. Carbohydr. Chem. Biochem.*, 1992, **49**, 93.

45. R. Storbeck, M. Ballauff. *J. Appl. Polym. Sci.*, 1996, **59**, 1199.

46. J.M. Aubry, Y. Zhu, V. Molinier, M. Durand, A. Lavergne. *Langmuir*, 2009, **25**, 13419.

47. L.A.M. Rupert. *J. Colloid Interface Sci.*, 1992, **153**, 92.